NIH Public Access
Author Manuscript
J Vet Cardiol. Author manuscript; available in PMC 2013 March 03.

Published in final edited form as:
J Vet Cardiol. 2012 March ; 14(1): 211–221. doi:10.1016/j.jvc.2012.02.006.

Interactions between TGFβ1 and cyclic strain in modulation of myofibroblastic differentiation of canine mitral valve interstitial cells in 3D culture

Andrew S. Waxman, DVM[a], **Bruce G. Kornreich, DVM, PhD**[a], **Russell A. Gould, BS, MS**[b], **N. Sydney Moïse, DVM, MS**[a], and **Jonathan T. Butcher, PhD**[b]

[a]Clinical Sciences, College of Veterinary Medicine, Cornell University, Ithaca NY 14853

[b]Biomedical Engineering, Cornell University, Ithaca, NY 14853

Abstract

Objectives—The mechanisms of myxomatous valve degeneration (MVD) are poorly understood. Transforming growth factor-beta1 (TGFβ1) induces myofibroblastic activation in mitral valve interstitial cells (MVIC) in static 2D culture, but the roles of more physiological 3D matrix and cyclic mechanical strain are unclear. In this paper, we test the hypothesis that cyclic strain and TGFβ1 interact to modify MVIC phenotype in 3D culture.

Animals, Materials and Methods—MVIC were isolated from dogs with and without MVD and cultured for 7 days in type 1 collagen hydrogels with and without 5 ng/ml TGFβ1. MVIC with MVD were subjected to 15% cyclic equibiaxial strain with static cultures serving as controls. Myofibroblastic phenotype was assessed via 3D matrix compaction, cell morphology, and expression of myofibroblastic (TGFβ3, alpha-smooth muscle actin - αSMA) and fibroblastic (vimentin) markers.

Results—Exogenous TGFβ1 increased matrix compaction by canine MVIC with and without MVD, which correlated with increased cell spreading and elongation. TGFβ1 increased αSMA and TGFβ3 gene expression, but not vimentin expression, in 15% cyclically stretched MVIC. Conversely, 15% cyclic strain significantly increased vimentin protein and gene expression, but not αSMA or TGFβ3. 15% cyclic strain however was unable to counteract the effects of TGFβ1 stimulation on MVIC.

Conclusions—These results suggest that TGFβ1 induces myofibroblastic differentiation (MVD phenotype) of canine MVIC in 3D culture, while 15% cyclic strain promotes a more fibroblastic phenotype. Mechanical and biochemical interactions likely regulate MVIC phenotype with dose dependence. 3D culture systems can systematically investigate these phenomena and identify their underlying molecular mechanisms.

Keywords

fibroblast; strain; myxomatous degeneration; tissue engineering; dog

© 2012 Elsevier B.V. All rights reserved.

Corresponding Author. Jtb47@cornell.edu (J.T. Butcher).

Conflict of Interests
The authors have no conflict of interest.

Publisher's Disclaimer: This is a PDF file of an unedited manuscript that has been accepted for publication. As a service to our customers we are providing this early version of the manuscript. The manuscript will undergo copyediting, typesetting, and review of the resulting proof before it is published in its final citable form. Please note that during the production process errors may be discovered which could affect the content, and all legal disclaimers that apply to the journal pertain.

$watermark-text

$watermark-text

$watermark-text

$watermark-text

$watermark-text

$watermark-text

Introduction

Mechanical stress and biochemical alterations can contribute to the phenotypic change of the mitral valve undergoing degeneration.[1,2] Understanding how these factors contribute to myxomatous valve disease (MVD) in the dog, demands exploration not only *in vivo*, but also through *in vitro* studies that permit specific examination of mechanical and signaling mechanisms. Mitral valve leaflets are highly organized, layered structures populated by interstitial cells (MVIC) that are responsible for developing and maintaining tissue stability and matrix architecture.[3,4] This stability and architecture is markedly destroyed in the myxomatous leaflets[5] Normally MVIC are fibroblastic in cytoskeletal phenotype, but promote a high degree of matrix turnover to support critically important valve function within their extremely demanding hemodynamic environment.[6] In both canine and human valves with MVD, MVIC transition to a myofibroblastic-like cell expressing contractile filaments such as alpha-smooth muscle actin (αSMA) and desmin.[7-9] The destruction of organized collagenous matrix in mitral valves with MVD, combined with deposition of glycosaminoglycans, results in significantly more compliant leaflet tissues, which is postulated to contribute to their insufficiency.[10] It is well known that mitral valve leaflets are subjected to multi-axial cyclic deformation during the cardiac cycle,[11,12] but how tissue mechanics contribute to canine MVIC phenotype and valve matrix remodeling is less clear.

Cytokines such as transforming growth factor beta (TGFβ) have been implicated in the pathogenesis of canine MVD.[13,14] Elevated TGFβ1-3 gene and protein expression have been found in canine mitral valves with MVD.[13,14] Components of serotonin metabolism are also differentially expressed in canine MVD,[15] which has been shown to modulate TGFβ signaling and myofibroblastic activation in sheep and porcine valve interstitial cells.[16]

Recent studies have shown that alterations in cyclic mechanical strain can lead to MVIC transformation to a myofibroblast-like, that is, MVD phenotype.[17,18] Cyclic stretch also alters glycosaminoglycan and proteoglycan profiles in porcine MVIC seeded collagen gels.[19-21] The amount of collagen and glycosaminoglycan synthesis has been shown to be dependent on the amplitude and frequency of stretch.[19-21] It has been suspected that extracellular matrix remodeling takes place in response to local mechanical stimuli and is mediated by TGFβ1.[22] Many of the strain induced effects can be reversed by TGFβ1 signaling blockade.[27] Merryman et al[17] demonstrated in porcine aortic valve interstitial cells that cyclic strain and exogenous TGFβ synergize to elevate collagen synthesis and TGFβ signaling. These findings suggest that cyclic mechanical strain and TGFβ signaling may act together to promote mitral valve remodeling, but whether and how this occurs in the context of canine MVD is unknown. In this study, we test the hypotheses that TGFβ1 and cyclic mechanical strain modulate myofibroblastic differentiation and matrix compaction by canine MVIC in 3-dimensional (3D) culture. We further probe the synergistic or antagonistic effects of strain and TGFβ on canine MVIC.

Methods

Tissue Collection and cell culture

Anterior mitral valve leaflets were collected from beagle dogs euthanized for reasons as part of institutionally approved *in vitro* studies unrelated to mitral valves. The dogs were healthy and had been given no medications. Specimens were classified as having either normal (n = 2) or mildly myxomatous (n = 2) degeneration via gross pathological inspection with the latter characterized by thickened, irregular leaflets and mitral regurgitation documented by echocardiography. Both dogs with MVD were 7 years of age while the normal dogs were 2 years of age. Cells from the normal dogs were used in the compaction studies alone. For all

$watermark-text

$watermark-text

$watermark-text

other studies only the cells from the myxomatous valves were used. Mitral valve interstitial cells were isolated from the non-chordal regions of each sample independently via collagenase digestion (Type II, 300 U/ml)[c] as previously described.[24] Cells were grown on tissue culture treated polystyrene and fed with Dulbecco's modified Eagle's medium (DMEM)[d] with 10% fetal bovine serum[e] and 1% penicillin/streptomycin[d]. Media was exchanged every 48 hours, and cells were passaged upon confluence. Cells were used in assays between passages 3 and 5.

Matrix Compaction

Trypsinized confluent MVIC (normal MIVIC or myxomatous MVIC) were pelleted via centrifugation and dispersed within neutralized type 1 collagen hydrogels[f] (2 mg/ml) at a concentration of 1×10^6 cells/ml as previously described.[25] The solution was inoculated into culture well plates, creating cylindrical gels of uniform initial area. After 1 hour of solidification, gels were released from their culture substrate and fed either culture media alone or media supplemented with 5 ng/ml of human recombinant TGFβ1[g]. Gels were then allowed to culture free-floating for 7 days, with digital images taken daily. From these images, hydrogel cross-section area was calculated using ImageJ[h]. Matrix compaction was then expressed as a ratio of final to original area.

Equibiaxial strain of MVIC hydrogels

Mitral valve leaflets *in vivo* experience a complex heterogeneous cyclic biaxial strain profile[26] that is difficult to impose *in vitro*. We approximated this strain environment using a novel cyclic strain bioreactor capable of stimulating engineered tissue models.[27] (Fig. 1) Briefly as we have described more thoroughly elsewhere,[27] cylindrical wells were fabricated within thick elastomeric silicone (1:10 ratio of catalyst:PDMS) slabs. These slabs were then affixed between two aluminum plates, leaving concentric circular openings below each well. The plates were then adhered to a stage whose vertical motion was controlled by a screw gear and rotary stepper motor. As the stage is raised and lowered, each well is stretched across a platen, creating a homogeneous equiaxial strain distribution with a sinusoidal time profile. The entire system is housed in a standard tissue culture incubator, which is maintained at 37C and 5% CO_2 throughout the culture period. For these experiments, 1×10^6 cells/ml were suspended in 3D collagen constructs as detailed above and 150 μl of solution was placed in each well. Each silicone elastomer well is lined by a stainless steel spring for stable but flexible adhesion of the hydrogel. After 1 hour of gel solidification, each well was supplemented with culture medium. Constructs were allowed to compact for an additional 24 hours without strain. Medium was changed at 24 hours and replaced with either standard medium or medium supplemented with 5 ng/ml of TGFβ1. For all strain experiments, 15% area strain (equibiaxial) at a frequency of 1 Hz was applied for 48 hours, with static cultures serving as controls.

Cell phenotype assessment

At the completion of experiments, myxomatous MVIC constructs were fixed in 4% polyformaldehyde. Cell morphology in response to cyclic strain in 3D culture was determined via phalloidin based f-actin filament staining as previously described,[29] using cell area and circularity as metrics.[11] Immunofluorescent antibody staining for αSMA and

[c]Worthington Biochemical Corp., Lakewood, NJ
[d]Invitrogen Corp., Grand Island, NY
[e]Hycel Inc., Houston, Tx
[f]Beckton-Dickinson, Franklin Lakes, NJ
[g]R&D Systems, Inc., Minneapolis, MN
[h]ImageJ NIH, Bethesda, MD

$watermark-text

$watermark-text

$watermark-text

vimentin protein expression indicated myofibroblastic or fibroblastic phenotypes as previously described.[28] Briefly, constructs were washed with phosphate buffered saline, then permeabilized with 0.2% Triton-X 100 for 10 minutes. Another wash with phosphate buffered saline was followed by overnight blocking with 1% bovine serum albumin kept at 4C. The blocking solution was aspirated and 1:100 dilutions of rabbit anti-vimentin and mouse anti-αSMA were added and incubated overnight at 4C. After additional washes, secondary antibodies (goat anti-mouse 568 and goat anti-rabbit 488) at 1:100 dilutions were added to constructs and incubated for 2 hours at room temperature. Draq5 was used at 1:1000 dilution as a DNA counterstain. Fluorescence was visualized utilizing confocal microscopy (Leica, LSM510).[i] Maximal projections of a stacked series of images (10 × 10 um) were created using Leica software.[i] The total number of cells was calculated by converting images to greyscale. The percentages of cells positive for vimentin and αSMA were obtained for each condition using ImageJ[h], with Draq5 positive nuclei as an indicator of total cells. Analyze particles were used to select each nucleus and count the total number of cells. Ratios were made for the number of cells positive for a particular protein to the total number of cells. Data was normalized to static controls.

Real-time PCR

Real-time PCR was conducted to assess gene expression changes in myxomatous MVIC with cyclic strain and/or TGFβ1. Primers for genes encoding proteins associated with myofibroblast phenotype (ACTA2, TGFβ3), fibroblast phenotype (vimentin), and a housekeeping gene (GAPDH) were designed using Primer3 (MIT) and validated using canine testicular cDNA (Table 1). After the conclusion of experiments, gels were lysed in RLT buffer and mRNA isolated using the RNEasy kit[j] according to the manufacturer's instructions and stored at -80C until use. cDNA was then created from mRNA using First Strand RT-PCR kit[d]. Real-time PCR amplification was achieved using the SYBR-green system[k] and read on an Optimax thermocycler[k]. The Livak method[k] ($\Delta\Delta C_T$ method) was used to calculate the fold change compared to GAPDH gene controls. Gene expression data was then expressed relative to unstrained gels cultured without TGFβ1. Confidence intervals for the point estimate of the fold change were calculated as previously described.[l]

Statistical analysis

3D compaction was compared between the normal and myxomatous MVIC, while the effects of strain, TGFβ1, and strain+TGFβ1 on ACTA2, TGFβ3 or vimentin expression was tested only in mildly myxomatous MVIC. Data are presented for these analyses with medians and ranges (median: range) and with dot-plots as applicable. For each of the multiple comparisons the Kruskal Wallis Test was used to determine if a difference existed between groups. The multiple comparisons included: (1) compaction between normal and myxomatous MVIC with and without TGFβ3), (2) area, circularity index, and (3) expression levels of ACTA2, TGF-β3, and vimentin under control, strain, TGFβ1, and strain/TGFβ1. If the Kruskal Wallis Test detected a significant difference in the multiple comparisons or for two nonpaired comparisons, analysis using a Mann-Whitney U test was performed with a Bonferroni correction for multiple comparisons.[m] For each of the 3 genes, we set the

[i]Leica Microsystems, Wetzlar, Germany
[j]Qiagen Inc., Valencia, CA
[k]Biorad Laboratories, Hercules, CA
[l]http://www3.appliedbiosystems.com/cms/groups/mcb_support/documents/generaldocuments/cms_042380 Applied Biosystems, 2008. Guide to performing relative quantitation of gene expression using real-time quantitative PCR. Part No. 4371095 Rev B.
[m]Analytical Software, Tallahassee FL

$watermark-text

$watermark-text

$watermark-text

comparison-wise α at 0.05. Publically available software was utilized for analysis (PAST).[n] The gene expressions are presented as fold differences +/- 95 % confidence intervals.

Results

Hydrogel compaction of normal and myxomatous canine MVIC

Canine MVIC compacted collagen hydrogels over the 7-day period, with final gel area 20-40% of original area depending on the experimental condition. As seen in Figure 2 the compaction (day 7 area/initial area) for the diseased MVIC hydrogels changes rapidly between days 2 and 3. At experimental endpoint of day 7 (Figure 2), myxomatous MVIC in the presence of TGFβ1 (n = 8) (0.179; 0.161 – 0.212) compacted hydrogels more than myxomatous MVIC without TGFβ1 (n = 7) (0.112; 0.109 – 0.118) (P = 0.005). The compaction by normal MVIC with TGFβ1 (n = 2) (0.323; 319 – 0.326) did not differ from that of normal MVIC without TGFβ1 (n = 5) (0.185; 0.179 – 0.221) with multiple pairwise comparisons, but the low numbers likely affected this analysis.

Effects of TGFβ1 and strain on myxomatous MVIC cell morphology

A total of 30 cells were measured per gel, with four hydrogels per treatment group, and 4 treatment groups were tested (120 cells per treatment). Cell size/structure was quantified via area and the circularity index[20] For the circularity index a value of 0 represented a line and a value of 1 represented a perfect circle. Collectively, the area of MVIC changed (P = 0.005) with TGFβ1 (290.54; 230.83 – 313.03 pixels), strain (63.02; 42.26 – 82.76 pixels), and TGFβ1 plus strain (155.65; 88.50 – 192.90 pixels) compared to that of MVIC with no TGFβ1 and no strain (67.04; 43.43 – 97.00 pixels), but post hoc pairwise comparisons could not identify a statistical difference among treatment groups. (Figure 3A) Moreover, the circularity index of MVIC changed (P = 0.02) with TGFβ1 (0.250; 0.238 – 0.283), strain (0.429; 0.356 – 0.622), and TGFβ1 plus strain (0.269; 0.240 – 0.288) compared to that of MVIC with no TGFβ1 and no strain (0.609; 0.499 – 0.665), but post hoc pairwise comparisons could not identify a statistical difference among treatment groups. (Figure 3B). This is likely due to the small number of hydrogels in each group (n = 4). Figures 3C and 3D illustrate why the median MVIC area is greater and the median MVIC circularity index is lower for MVIC cells treated with TGFβ1 than without TGFβ1. That is, without TGFβ1 the MVIC in 3D culture did not have an elongated morphology, but were more polygonal with a random orientation (Figure 3C). When treated with 5 ng/ml TGFβ1, MVIC appear larger and elongated, with filipodia like processes extending from the polar ends of the cells with a random orientation (Figure 3D).

Effects of TGFβ1 and strain on myxomatous MVIC protein and gene expression

In static 3D culture, MVIC expressed both vimentin and αSMA (Fig. 4). Unfortunately, an insufficient number of TGFβ1 treated samples stained properly for protein expression quantification. However, we did find that as a result of strain, vimentin protein expression significantly increased (P = 0.026) (0.837; 0.758 – 0.871 versus 0.658; 0.512 – 0.728 % in non-strained), while αSMA protein expression was unchanged (P = 0.68) (0.556; 0.535 – 0.631 versus 0; 0.438 – 0.594 % in non-strained) (Fig. 3B and 3C). Collectively, these findings suggest that mildly myxomatous MVIC are somewhat myofibroblast-like in static 3D culture, but that 15% cyclic equibiaxial strain promotes fibroblast-like differentiation.

Compared with static controls (n = 7) alterations in gene expression of ACTA2 (gene for protein αSMA), TGFβ3, and vimentin were observed when cyclic strain (n = 5), TGFβ1 (n

[n] http://folk.uio.no/ohammer/past. Hammer O, Harper DAT and Ryan PD, 2001. PAST: Paleontological Statistics software package for education and data analysis. Palaeontologia Electronica 4(1):9.

= 8), or both (n = 8) were applied to 3D cultures. (Figure 5, Table 2) ACTA2 expression did not differ from control in TGFβ1 or strain plus TGFβ1 treated 3D cultures; however, TGFβ increased ACTA2 expression when compared to cells subjected to cyclic strain alone (P = 0.04). The expression of TGFβ3 with only cyclic strain applied was insignificantly less than control, but the expression of TGFβ3 was significantly increased with exogenous TGFβ1 administration both with (P = 0.009) and without (P = 0.02) cyclic strain. Strain did not alter TGFβ3 expression and the application of strain did not inhibit the expression of more TGFβ3 when treated with TGFβ1. Expression of vimentin was significantly enhanced by strain alone (P = 0.03), but not by TGFβ1 alone. In fact, when 3D cultures were treated with both TGFβ1 and cyclic strain, the expression of vimentin was significantly reduced compared to that observed in 3D cultures treated with strain alone.

Discussion

Our findings suggest that 5ng/ml TGFβ1 promotes transdifferentiation of canine MVIC to a myofibroblast phenotype in 3D cultures as assayed by functional collagen gel compaction, cell morphology, and gene expression of αSMA, and TGFβ3. The functional effects as assessed by compaction studies of TGFβ1 on canine MVIC phenotype appear similar in normal canine MVIC and MVIC obtained from dogs with MVD, although these effects appear to be more profound in myxomatous MVIC. Matrix compaction is driven primarily by cell-mediated traction forces.[29] Our results indicate that normal MVIC treated with TGFβ1 exert similar traction forces than myxomatous MVIC without TGFβ1. In addition, we have shown that 15% cyclic equibiaxial strain induces a transformation of canine MVIC to a fibroblast phenotype in 3D cultures, as assayed by protein expression of vimentin and αSMA and cell morphology. Finally, our results suggest that although cyclic strain may temper the morphologic response induced by TGFβ on canine MVIC, the effect of TGFβ1 on canine MVIC phenotype dominate that of cyclic strain. These findings validate our experimental model as a means of investigating the biochemical and mechanical influences on canine MVIC phenotype and provide insight into the interaction of strain and TGFβ1 on canine MVIC in 3D culture.

Canine MVD is a complex disease that is similar in many respects to MVD in humans.[30] Discovering the molecular and physical mechanisms that promote the transition from normal valves to pathological mitral valve disease in dogs is therefore an important research effort. The use of 3D matrix culture systems is important in recapitulating perhaps more physiological cell-matrix interactions that are vital to valve cell function.[25,31] In this study, we employ 3D collagen hydrogels to create 3D culture models of mitral valve tissues using canine MVIC. Matrix compaction is a function of active cell contraction [32,33] and cell traction forces associated with migration.[34] Our results suggest that myxomatous MVIC have enhanced migratory and/or traction force generation capacity. A number of studies suggest that contractile protein expression increases in MVIC obtained from diseased valves *in situ*, but traction forces were not addressed in these studies.[9] Furthermore, myxomatous MVIC appear to have increased expression of TGFβ family member receptors, which, from the standpoint of our results, supports an increased traction force generation leading to matrix compaction.[2,35] Because pathogenic valve cell differentiation and matrix remodeling *in vivo* is time dependent and heavily influenced by hemodynamic microenvironment,[36] we can't yet establish the complete picture. Our results however suggest that changes in cell phenotype and matrix composition are not co-incident, but sequential and likely evolving in a complex feedback.

The results of our study indicate that 15% cyclic equibiaxial strain promotes a more fibroblastic phenotype in mildly diseased MVIC. The addition of TGFβ1 however caused significant increases in expression of TGFβ3 and αSMA mRNA in both static and strained

$watermark-text $watermark-text $watermark-text

$watermark-text

$watermark-text

$watermark-text

cultures. These findings suggest that MVIC are responsive to both biomechanical and biochemical stimuli. Under these experimental conditions, strain and TGF-β1 acted antagonistically. The actual strain profiles in native mitral valves may be more biaxial in nature, but heavily heterogeneous.[26] Early MVD is characterized by focal lesions on the anterior leaflet in both dog and human, which suggests that local tissue strain patterns may promote or protect valve cells from differentiation. An analysis of mitral valve chordae and anterior leaflets suggests that diseased tissue is biomechanically weaker,[10] but direct correlations between local matrix composition and tissue mechanics are still lacking. These findings suggest that resident cells may experience greater strain magnitudes in diseased configurations. In aortic valves, tissue strain magnitudes over 20% appear to induce pathological cell differentiation and matrix remodeling, while 10-15% strains are protective.[37,38] Furthermore, Merryman et al[17] has shown that strain synergizes with TGFβ1 stimulation resulting in additional TGFβ stimulation and cell differentiation. Uniaxial stretch was applied to whole leaflets in that study, which differs significantly from our studies.[17] We employed equibiaxial strain because it is a completely uniform strain field, whereas uniaxial stretch imparts locally varying transverse strains. Our findings suggest that 15% cyclic strain was protective against myofibroblastic differentiation of MVIC, but strain magnitude and degree of anisotropy likely also affect mitral valve homeostasis and pathogenesis, alone and in combination with biochemical signaling. Additional studies are therefore required to dissect how each mode of stimulation influences MVIC phenotype and downstream matrix remodeling.

In vivo studies have suggested that increased contractility may alter the progression of MMVD in dogs with mild disease.[38] Hypothetically, the altered mechanical environment in this situation may alter strain and therefore induce a more myxomatous phenotype. However, cyclic strain imposed in our studies proved to be protective of the myxomatous phenotype. This suggests an interesting possibility with regards to the severity of myxomatous disease seen in dogs of different sizes and ages. Hypothetically, the variation in the clinical expression of the disease may be due not only to genetic variation for the substrate of the disease, but also the differences in strain on the valve leaflets in different dogs may be a factor for consideration in understanding the phenotypic variation. In a sheep model of papillary muscle tethering induced mitral valve stretch, tissue elongation and matrix remodeling with increased expression of αSMA was found primarily on the tensile loaded atrialis surface, which suggests that mechanical forces independent of pharmacologic stimulation may also drive MV pathogenesis.[36]

It is important to note the limitations in our study. First, we are studying a complex phenomenon in a simplified model. Certainly, *in vitro* mechanical studies cannot reproduce the multitude of factors present *in vivo:* however, our 3D culture system enables decoupling and direct testing of the mechanical and biochemical alterations that are involved in the degenerative process that cannot be studied *in vivo.* Furthermore, while our analysis includes gene, protein, and functional readouts of the fibroblastic-myofibroblastic phenotype axis of MVIC, it is by no means an exhaustive list. Due to limited numbers of cells isolated from diseased dogs and our desire to maintain low passage number, we were unable to test the full comparison sets of strain versus TGFβ1. Our experimental endpoints of 48 hours for cell phenotype and seven days for matrix compaction are standard in the literature, but it is clear from Figure 1 that cell induced remodeling of collagen gels is time dependent.

Conclusions

These results support that TGFβ1 induces myofibroblastic differentiation (MVD phenotype) of canine MVIC in 3D culture, while 15% cyclic strain promotes a more fibroblastic phenotype. 3D culture of canine MVIC permits focused studies to increase our knowledge

on the mechanical and biochemical changes that may be involved in the cellular phenotype of MVD.

Acknowledgments

We appreciate the statistical consultation and valuable assistance of Dr. Mark Rishniw. We are very grateful for the technical expertise and helpful discussions with Dr. Eva Oxford. This study was supported by a grant from the ACVIM subspecialty of Cardiology Resident Research Grant Support a National Science Foundation CAREER Award (CBET – 0955172), the American Heart Association (Scientist Development Grant #0830384N), the National Institutes of Health (HL110328), and the Leducq Foundation (Project MITRAL).

References

1. Richards JM, Farrar EJ, Kornreich BG, Moïse NS, Butcher J. The mechanobiology of mitral valve function, degeneration, and repair. 2012; 14:xxx–xxx.
2. Rabkin E, Aikawa M, Stone JR, Fukumoto Y, Libby P, Schoen FJ. Activated interstitial myofibroblasts express catabolic enzymes and mediate matrix remodeling in myxomatous heart valves. Circulation. 2001; 104:2525–2533. [PubMed: 11714645]
3. Liu AC, Joag VR, Gotlieb AI. The emerging role of valve interstitial cell phenotypes in regulating heart valve pathobiology. Am J Pathol. 2007; 171:1407–1418. [PubMed: 17823281]
4. Hinton RB Jr, Lincoln J, Deutsch GH, Osinska H, Manning PB, Benson DW, Yutzey KE. Extracellular matrix remodeling and organization in developing and diseased aortic valves. Circ Res. 2006; 98:1431–1438. [PubMed: 16645142]
5. Fox PR. Pathology of myxomatous mitral valve *1* disease in the dog. J Vet Cardiol. 2012; 14:xxx–xxx.
6. Schneider PJ, Deck JD. Tissue and cell renewal in the natural aortic valve of rats: an autoradiographic study. Cardiovasc Res. 1981; 15:181–189. [PubMed: 7273050]
7. Han RI, B A, Culshaw GJ, French AT, Else RW, Corcoran BM. Distribution of myofibroblasts, smooth muscle-like cells, macrophages, and mast cells, in mitral valve leaflets of dogs with myxomatous mitral valve disease. Am J Vet Res. 2008; 69:763–769. [PubMed: 18518656]
8. Disatian S, Ehrhart EJ 3rd, Zimmerman S, Orton EC. Interstitial cells from dogs with naturally occurring myxomatous mitral valve disease undergo phenotype transformation. J Heart Valve Dis. 2008; 17:402–411. [PubMed: 18751470]
9. Rabkin-Aikawa E, Farber M, Aikawa M, Schoen FJ, Source D. Dynamic and reversible changes of interstitial cell phenotype during remodeling of cardiac valves. J Heart Valve Dis. 2004; 13:841–847. [PubMed: 15473488]
10. Barber JE, Kasper FK, Ratliff NB, Cosgrove DM, Griffin BP, Vesely I. Mechanical properties of myxomatous mitral valves. J Thorac Cardiovasc Surg. 2001; 122:955–962. [PubMed: 11689801]
11. Grashow JS, Sacks MS, Liao J, Yoganathan AP. Planar biaxial creep and stress relaxation of the mitral valve anterior leaflet. Ann Biomed Eng. 2006; 34:1509–1518. [PubMed: 17016761]
12. Liao J, Yang L, Grashow J, Sacks MS. The relation between collagen fibril kinematics and mechanical properties in the mitral valve anterior leaflet. J Biomech Eng. 2007; 129:78–87. [PubMed: 17227101]
13. Oyama MA, Chittur SV. Genomic expression patterns of mitral valve tissues from dogs with degenerative mitral valve disease. Am J Vet Res. 2006; 67:1307–1318. [PubMed: 16881841]
14. Zheng J, Chen Y, Pat B, Dell'Italia LA, Tillson M, Dillon AR, Powell PC, Shi K, Shah N, Denney T, Husain A, Dell'Italia LJ. Microarray identifies extensive downregulation of noncollagen extracellular matrix and profibrotic growth factor genes in chronic isolated mitral regurgitation in the dog. Circulation. 2009; 119:2086–2095. [PubMed: 19349319]
15. Disatian S, Orton EC. Autocrine serotonin and transforming growth factor beta 1 signaling mediates spontaneous myxomatous mitral valve disease. J Heart Valve Dis. 2009; 18:44–51. [PubMed: 19301552]
16. Jian B, Xu J, Connolly J, Savani RC, Narula N, Liang B, Levy RJ. Serotonin mechanisms in heart valve disease I: serotonin-induced up-regulation of transforming growth factor-beta1 via G-protein

$watermark-text
$watermark-text
$watermark-text

$watermark-text

$watermark-text

$watermark-text

signal transduction in aortic valve interstitial cells. Am J Pathol. 2002; 161:2111–2121. [PubMed: 12466127]

17. Merryman WD, Lukoff HD, Long RA, Engelmayr GC Jr, Hopkins RA, Sacks MS. Synergistic effects of cyclic tension and transforming growth factor-beta1 on the aortic valve myofibroblast. Cardiovasc Pathol. 2007; 16:268–276. [PubMed: 17868877]
18. Butcher JT, Nerem RM. Valvular endothelial cells regulate the phenotype of interstitial cells in co-culture: effects of steady shear stress. Tissue Eng. 2006; 12:905–915. [PubMed: 16674302]
19. Ku CH, Johnson PH, Batten P, Sarathchandra P, Chambers RC, Taylor PM, Yacoub MH, Chester AH. Collagen synthesis by mesenchymal stem cells and aortic valve interstitial cells in response to mechanical stretch. Cardiovasc Res. 2006; 71:548–556. [PubMed: 16740254]
20. Gupta V, Tseng H, Lawrence BD, Grande-Allen KJ. Effect of cyclic mechanical strain on glycosaminoglycan and proteoglycan synthesis by heart valve cells. Acta Biomater. 2009; 5:531–540. [PubMed: 19004676]
21. Balachandran K, Konduri S, Sucosky P, Jo H, Yoganathan AP. An ex vivo study of the biological properties of porcine aortic valves in response to circumferential cyclic stretch. Ann Biomed Eng. 2006; 34:1655–1665. [PubMed: 17031600]
22. Lee AA, Delhaas T, McCulloch AD, Villarreal FJ. Differential responses of adult cardiac fibroblasts to in vitro biaxial strain patterns. J Mol Cell Cardiol. 1999; 31:1833–1843. [PubMed: 10525421]
23. Li Q, Muragaki Y, Hatamura I, Ueno H, Ooshima A. Stretch-induced collagen synthesis in cultured smooth muscle cells from rabbit aortic media and a possible involvement of angiotensin II and transforming growth factor-beta. J Vasc Res. 1998; 35:93–103. [PubMed: 9588872]
24. Butcher JT, Nerem RM. Valvular endothelial cells regulate the phenotype of interstitial cells in co-culture: effects of steady shear stress. Tissue Eng. 2006; 12:905–915. [PubMed: 16674302]
25. Butcher JT, Nerem RM. Porcine aortic valve interstitial cells in three-dimensional culture: comparison of phenotype with aortic smooth muscle cells. J Heart Valve Dis. 2004; 13:478–485. [PubMed: 15222296]
26. Sacks MS, Enomoto Y, Graybill JR, Merryman WD, Zeeshan A, Yoganathan AP, Levy RJ, Gorman RC, Gorman JH 3rd. In-vivo dynamic deformation of the mitral valve anterior leaflet. Ann Thorac Surg. 2006; 82:1369–1377. [PubMed: 16996935]
27. Gould RA, Chin K, Santisakultarm TP, Dropkin A, Richards JM, Schaffer CB, Butcher JT. Cyclic strain anisotropy regulates valvular interstitial cell phenotype and tissue remodeling in three-dimensional culture. Acta Biomaterialia. 2012; xxx:xxx–xxx.
28. Butcher JT, Barrett BC, Nerem RM. Equibiaxial strain stimulates fibroblastic phenotype shift in smooth muscle cells in an engineered tissue model of the aortic wall. Biomaterials. 2006; 27:5252–5258. [PubMed: 16806457]
29. Tranquillo RT, Durrani MA, Moon AG. Tissue engineering science: consequences of cell traction force. Cytotechnology. 1992; 10:225–250. [PubMed: 1369238]
30. Pomerance A, Whitney JC. Heart valve changes common to man and dog: a comparative study. Cardiovasc Res. 1970; 4:61–66. [PubMed: 5416844]
31. Gupta V, Werdenberg JA, Blevins TL, Grande-Allen KJ. Synthesis of glycosaminoglycans in differently loaded regions of collagen gels seeded with valvular interstitial cells. Tissue Eng. 2007; 13:41–49. [PubMed: 17518580]
32. El-Hamamsy I, Balachandran K, Yacoub MH, Stevens LM, Sarathchandra P, Taylor PM, Yoganathan AP, Chester AH. Endothelium-dependent regulation of the mechanical properties of aortic valve cusps. J Am Coll Cardiol. 2009; 53:1448–1455. [PubMed: 19371829]
33. Grinnell F, Ho CH, Lin YC, Skuta G. Differences in the regulation of fibroblast contraction of floating versus stressed collagen matrices. J Biol Chem. 1999; 274:918–923. [PubMed: 9873032]
34. Soini Y, Satta J, Maatta M, Autio-Harmainen H. Expression of MMP2, MMP9, MT1-MMP, TIMP1, and TIMP2 mRNA in valvular lesions of the heart. J Pathol. 2001; 194:225–231. [PubMed: 11400152]
35. Dal-Bianco JP, Aikawa E, Bischoff J, Guerrero JL, Handschumacher MD, Sullivan S, Johnson B, Titus JS, Iwamoto Y, Wylie-Sears J, Levine RA, Carpentier A. Active adaptation of the tethered

mitral valve: insights into a compensatory mechanism for functional mitral regurgitation. Circulation. 2009; 120:334–342. [PubMed: 19597052]

36. Smith KE, Metzler SA, Warnock JN. Cyclic strain inhibits acute pro-inflammatory gene expression in aortic valve interstitial cells. Biomech Model Mechanobiol. 2010; 9:117–125. [PubMed: 19636599]
37. Balachandran K, Hussain S, Yap CH, Padala M, Chester AH, Yoganathan AP. Elevated cyclic stretch and serotonin result in altered aortic valve remodeling via a mechanosensitive 5-HT(2A) receptor-dependent pathway. Cardiovasc Pathol. 2011 Epub ahead of print.
38. Chetboul V, Lefebvre HP, Sampedrano CC, Gouni V, Saponaro V, Serres F, Concordet D, Nicolle AP, Pouchelon JL. Comparative adverse cardiac effects of pimobendan and benazepril monotherapy in dogs with mild degenerative mitral valve disease: A prospective, controlled, blinded, and randomized study. J Vet Intern Med. 2007; 21:742–753. [PubMed: 17708394]

Abbreviations

3D	3-dimensional
MVD	Myxomatous valve degeneration
MVIC	Mitral valve interstitial cells
αSMA	Alpha-smooth muscle actin
TGFß1-3	Transforming growth factor-beta1-3

$watermark-text
$watermark-text
$watermark-text

$watermark-text
$watermark-text
$watermark-text

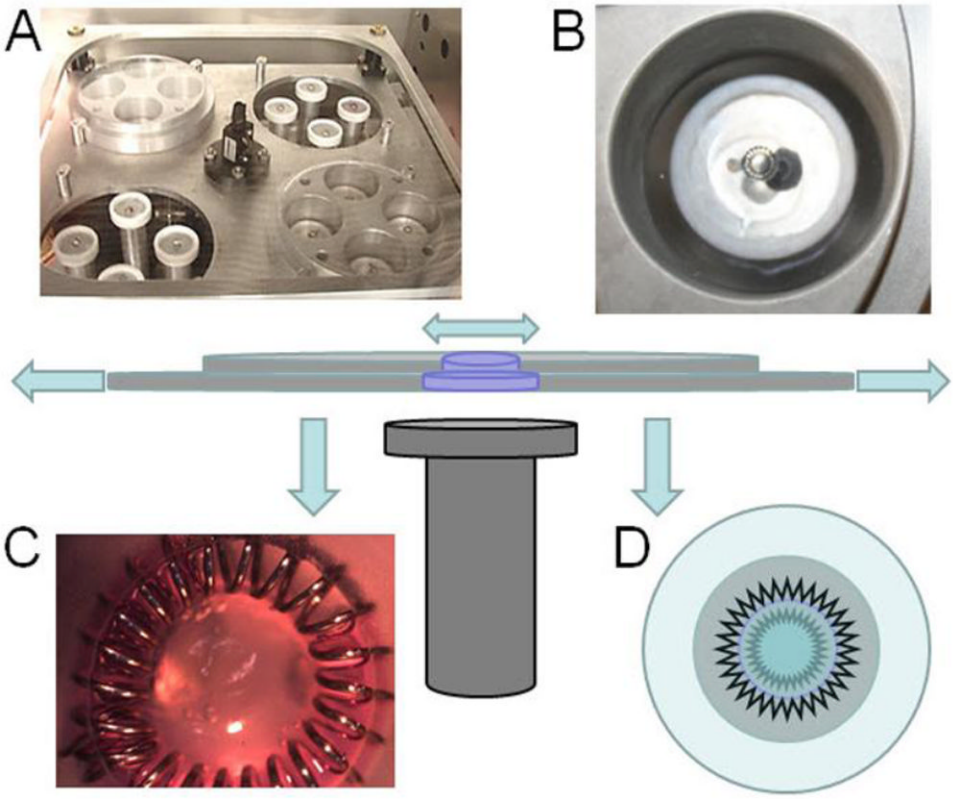

Figure 1.
System for cyclic equibiaxial strain of 3D cultured cells. A) Translation stage containing 4 cylindrical cassettes (e.g. top left and bottom right) each with 4 holes concentric above circular platens (B). The cassettes sandwich a thick slab of elastomeric material, within which small partial depth wells are created (C) into which a hydrogel is cast. The hydrogel containing cells is anchored by means of a spring steel ring that flexes as the well is stretched, thus stretching the gel (D). In D the inner jagged ring symbolizes the nonstretched hydrogel and the outer jagged ring the stretched. The central schematic demonstrates the mechanism of cyclic stage translation and gel stretch. See Gould et al, Acta Biomaterialia 2012, for more details.

$watermark-text
$watermark-text
$watermark-text

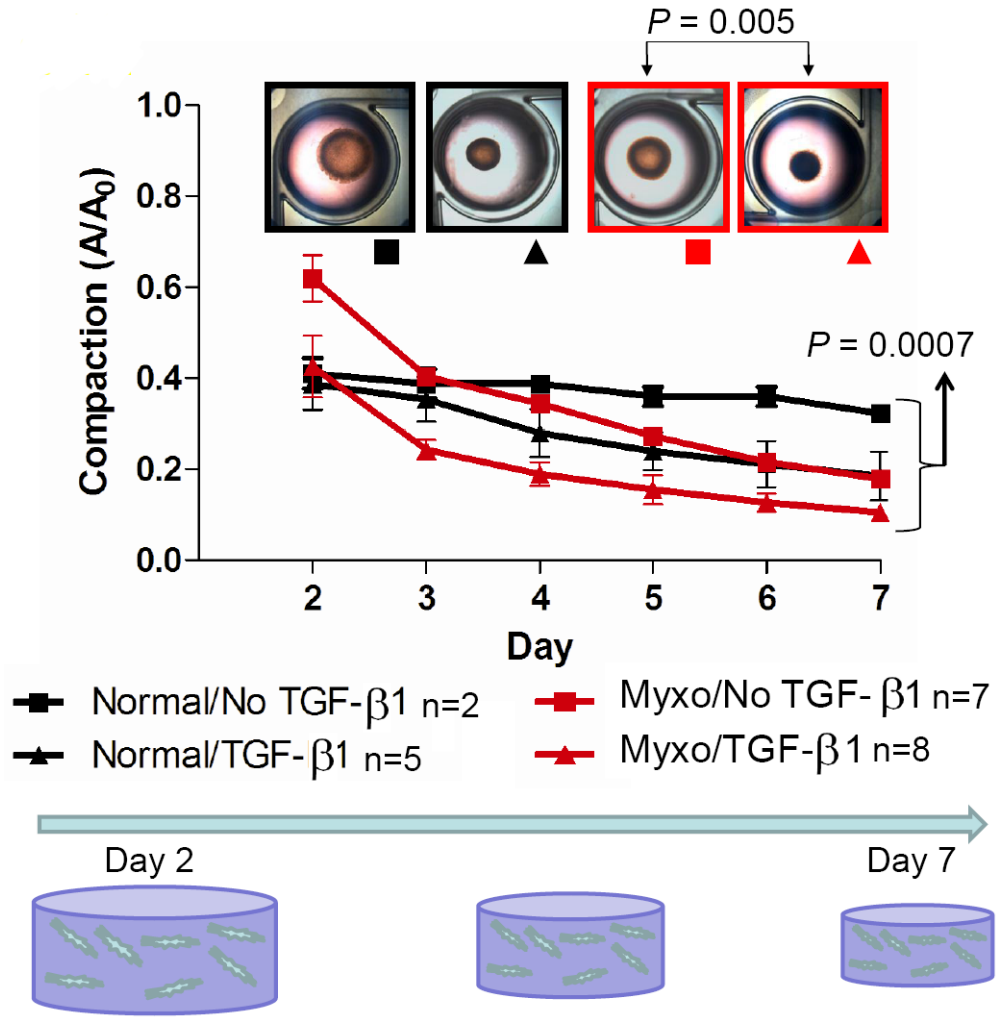

Figure 2.

Compaction of 3D hydrogels by mitral valve interstitial cells (MVIC) from normal valves and valves with mild myxomatous degeneration. Gels of each cell source were cultured with or without TGFß1. Compaction was quantified as projected area with respect to original (Day 0) area. A significant compaction amongst the groups was noted at day 7 with the pairwise comparisons revealing a significant difference only between the treated and nontreated myxomatous cell hydrogels

$watermark-text

$watermark-text

$watermark-text

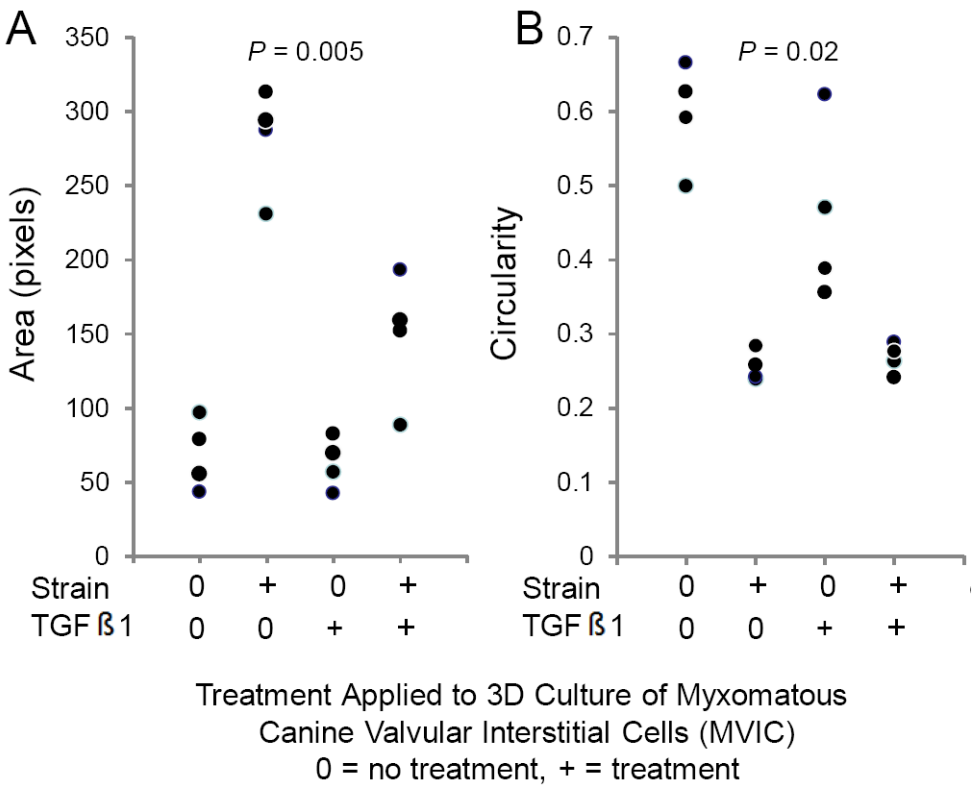

$watermark-text

$watermark-text

$watermark-text

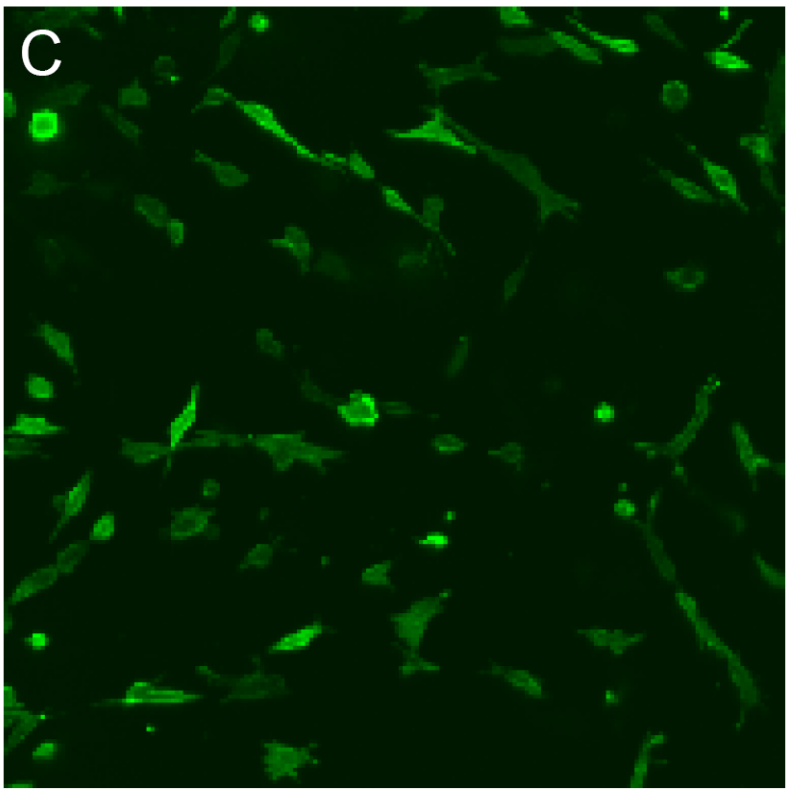

No TGF-β1

$watermark-text

$watermark-text

$watermark-text

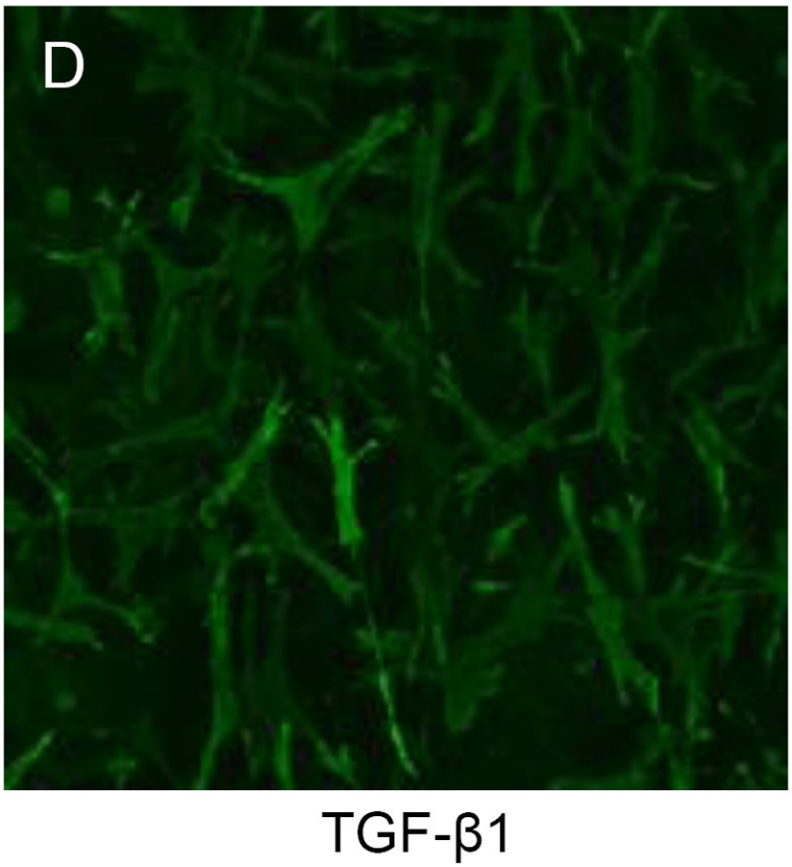

Figure 3.
TGFβ1 alters morphology of myxomatous MVIC in 3D culture. Dot-plots of area (A) and circularity index (B) show changes with 15% cyclic strain and TGFβ1. (C,D): Immunofluorescent images of 3D culture cell morphology (via f-actin) without (C) and with (D) TGFβ1.

$watermark-text
$watermark-text
$watermark-text

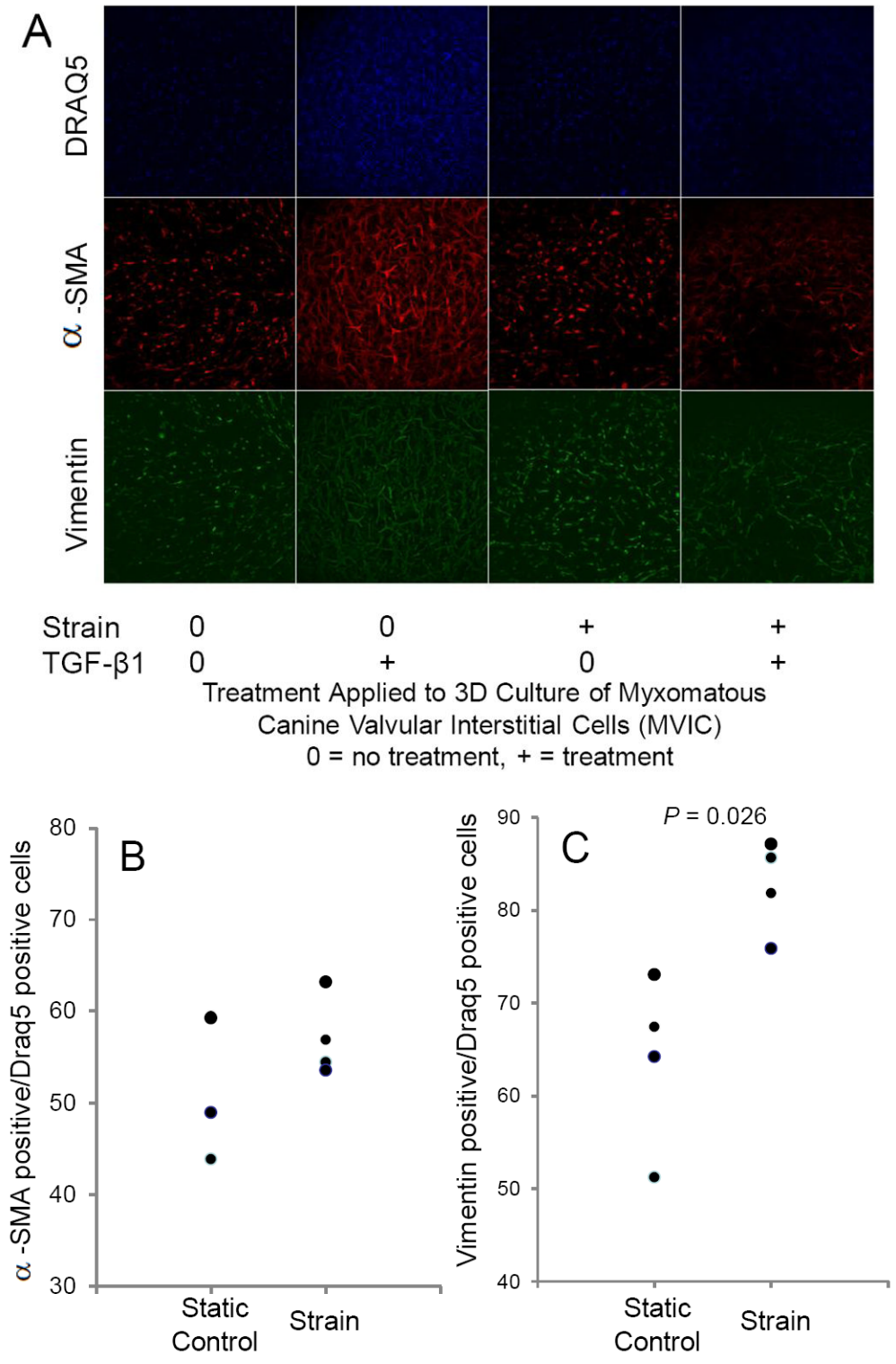

Figure 4.

Protein expression changes in canine MVIC with cyclic stretch and/or TGFβ1. (A) Immunofluorescent staining for alpha-smooth muscle actin (αSMA, red), vimentin (green), and DNA (blue) in MVIC cultured in 3D hydrogels. Cells were from 3D cultures that were

under static control conditions (0,0), treatment with TGFβ1 alone (0,+), 15% cyclic strain alone (+,0) or both TGFβ1 and strain (+,+). Cells expressing αSMA (B) and vimentin (C) were quantified and normalized to total cell number.

$watermark-text

$watermark-text

$watermark-text

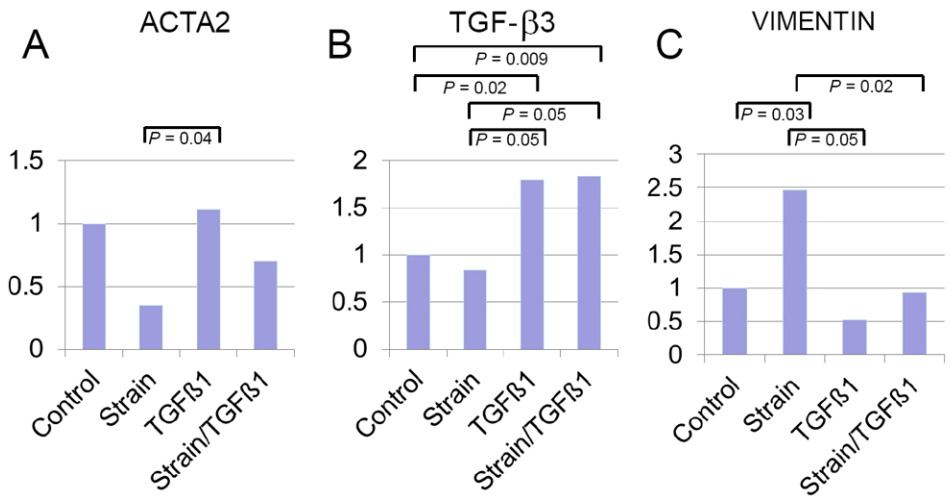

Figure 5.

Gene expression of ACTA2 (A), TGFβ3 (B), and vimentin (C) under static control conditions (n = 7), under biaxial cyclic strain alone (n = 5), with TGFβ1 alone (n = 8), and treated with both strain and TGFβ1 (n = 8). Data was normalized to GAPDH and expressed as fold difference from control. Bars denote statistically significant comparisons.

$watermark-text
$watermark-text
$watermark-text

$watermark-text

$watermark-text

$watermark-text

Table 1

Primers for canine genes encoding proteins associated with myofibroblast phenotype (ACTA2, TGFβ3), fibroblast phenoptype (vimentin), and housekeeping gene (GAPDH) used in this study.

Gene	Primer Sequence	Product Length (bp)
GAPDH	5’-TGGCAAAGTGGATATTGTCG-3’ 3’-AGATGGACTTCCCGTTGATG-5’	149
Vimentin	5’-TGGCAAAGTGGATATTGTCG-3’ 3’-AGATGGACTTCCCGTTGATG-5’	150
ACTA2	5’-CCCAGACATCAGGGAGTGAT-3’ 3’-CTTTTCCATGTCGTCCCAGT-5’	141
TGFβ3	5’-CTTGCACCACCTTGGACTTT-3’ 3’-CTGTTGTAAAGGGCCAGGAC-5’	148

$watermark-text

$watermark-text

$watermark-text

Table 2

Fold gene expression changes for myofibroblast-like (ACTA2, TGFβ3) and fibroblast-like phenotype (vimentin).

Gene	Condition	Fold Change*
ACTA2	Cyclic strain	0.35 (0.07-1.64)
ACTA2	TGFβ1	1.12 (0.15-2.99)
ACTA2	Cyclic strain + TGFβ1	0.52 (0.24-2.00)
TGFβ3	Cyclic strain	0.84 (0.31-2.29)
TGFβ3	TGFβ1	1.80 (0.73-4.48)
TGFβ3	Cyclic strain + TGFβ1	1.83 (1.18-2.85)
Vimentin	Cyclic strain	0.53 (0.17-1.6)
Vimentin	TGFβ1	2.47 (1.39-4.41)
Vimentin	Cyclic strain + TGFβ1	0.93 (0.53-1.65)

* Fold change with upper and lower 95% confidence intervals in parentheses